

# We are IntechOpen, the world's leading publisher of Open Access books Built by scientists, for scientists

6,900

Open access books available

186,000

International authors and editors

200M

Downloads

Our authors are among the

154

Countries delivered to

TOP 1%

most cited scientists

12.2%

Contributors from top 500 universities



WEB OF SCIENCE™

Selection of our books indexed in the Book Citation Index  
in Web of Science™ Core Collection (BKCI)

Interested in publishing with us?  
Contact [book.department@intechopen.com](mailto:book.department@intechopen.com)

Numbers displayed above are based on latest data collected.  
For more information visit [www.intechopen.com](http://www.intechopen.com)



---

# Application and Challenges of Signal Processing Techniques for Lamb Waves Structural Integrity Evaluation: Part A-Lamb Waves Signals Emitting and Optimization Techniques

---

Zenghua Liu and Honglei Chen

Additional information is available at the end of the chapter

<http://dx.doi.org/10.5772/intechopen.78381>

---

## Abstract

Lamb waves have been widely studied in structural integrity evaluation during the past decades with their low-attenuation and multi-defects sensitive nature. The performance of the evaluation has close relationship with the vibration property and the frequency of Lamb waves signals. Influenced by the nature of Lamb waves and the environment, the received signals may be difficult to interpret that limits the performance of the detection. So pure Lamb waves mode emitting and high-resolution signals acquisition play important roles in Lamb waves structural integrity evaluation. In this chapter, the basic theory of Lamb waves nature and some environment factors that should be considered in structural integrity evaluation are introduced. Three kinds of typical transducers used for specific Lamb waves mode emitting and sensing are briefly introduced. Then the development of techniques to improve the interpretability of signals are discussed, including the waveform modulation techniques, multi-scale analysis techniques and the temperature effect compensation techniques are summarized.

**Keywords:** Lamb waves, plate, transducers, signal optimization techniques, structural integrity evaluation

---

## 1. Introduction

Plate-like structures made with metallic and composite materials have been widely used in various of engineering fields including aerospace and civil engineering. During the manufacturing, processing and usage, various type of damage may be induced in these structures. For

---

example, corrosion and fatigue cracks are common defects in metal plates, while the main defects in composite plates are delamination, debonding, etc. Thus, it is important to develop defects detection and monitoring techniques to ensure the integrity of plate structures. Lamb waves have multi-modes, full cross-section distribution and low-attenuation nature in plates and can be used for multi-type defects detection in large scale. Combined with modern signal detection instruments and signal processing techniques, there are a lot of research and application of Lamb waves for off-line and on-line structure integrity evaluation [1–3].

Lamb waves are a type of elastic waves that remain the constraint between two parallel free surfaces, such as the upper and lower surfaces of a plate or shell, which contribute both longitudinal and shear partial wave components, as shown in **Figure 1(a)**. According to the particle vibration mode, mainly two kinds of Lamb waves modes are formed as the interaction of longitudinal and shear partial waves, symmetric (S) modes and anti-symmetric (A) modes shown in **Figure 1(b)**. Lamb waves theory, which is fully documented in literatures [4–6], assumes the derivation formula in a cylindrical coordinate of the three-dimensional (3D) waves as

$$\begin{cases} \frac{\partial^2 \phi}{\partial x^2} + \frac{\partial^2 \phi}{\partial y^2} + \frac{\omega^2}{c_l^2} \phi = 0 \\ \frac{\partial^2 \psi}{\partial x^2} + \frac{\partial^2 \psi}{\partial y^2} + \frac{\omega^2}{c_s^2} \psi = 0 \end{cases}, \quad (1)$$

where  $\phi$  and  $\psi$  are potential functions,  $c_l^2 = (\lambda + 2\mu)/\rho$  and  $c_s^2 = \mu/\rho$  are the longitudinal and shear wave velocities, respectively,  $\lambda$  and  $\mu$  are the Lamé constants and  $\rho$  is the mass density.

Under the stress-free boundary conditions at the upper and lower surfaces, Lamb waves equation can be obtained with the separation variable solution method

$$\frac{\tan \beta d}{\tan \alpha d} = - \left[ \frac{4k^2 \alpha \beta}{(k^2 - \beta^2)^2} \right]^{\pm 1}, \quad (2)$$

where  $d$  is the half thickness of plates,  $k$  is the wavenumber,  $k^2 = \omega^2/c_p^2$ ,  $c_p$  is the phase velocity,  $\alpha^2 = \omega^2/c_l^2 - k^2$ ,  $\beta^2 = \omega^2/c_s^2 - k^2$ . The plus sign corresponds to symmetric vibration and the minus to anti-symmetric vibration. A series of eigenvalues  $k_i^S$  and  $k_i^A$  corresponding various Lamb waves mode shapes are obtained by solving Eq. (2). The S modes and A modes are denoted with  $S_i$  and  $A_i$ , respectively, where the subscript  $i$  indicates the order of the modes and equals 0,1,2,... The relationship  $c_p = \omega/k$  yields the dispersive wave velocity which is a function of the product between the frequency and the plate thickness. The wavelength is defined as  $\lambda = c_p/f$ . The group velocity,  $c_g$ , can be derived from the phase velocity with

$$c_g = c_p^2 \left( c_p - f d \frac{\partial c_p}{\partial (fd)} \right)^{-1}. \quad (3)$$

**Figure 1(c)** and **(d)** shows dispersion curves of Lamb waves in an aluminum plate drawn with DISPERSE. The mechanical property of the plate is defined as: the density is 2.7 g/cm<sup>3</sup>,

Young's module is 70.753 GPa and Poisson's ratio is 0.33. It is easy to find that the particle vibration show out anti-symmetric and symmetric forms for A modes and S modes, respectively. As shown in **Figure 1(c)** and **(d)**, there are at least four modes under the frequency-thickness 8.0 MHz-mm including the fundamental modes ( $A_0$  and  $S_0$ ). The group velocities and the wavenumbers change with frequency for these Lamb waves modes, termed the dispersion nature of Lamb waves.

Defects in structures induce the scattering profiles and cause the change of the velocity and attenuation in the magnitude of Lamb waves signals. Besides the defects, there are still many other factors may induce the vibration, interpretability of the received Lamb waves signals in structural integrity evaluation. These factors are the Lamb waves nature, the property of transducers and plate structures, the environmental and operational conditions. Some of the influence by these factors is expressed below.

1. Dispersion of Lamb waves complexes the received signals that induce the signals extension in both spatial and temporal domain; multi-modes of Lamb waves and echoes from the multi-defects cause the waveform overlapping in received signals.
2. Property of the transducers influences the performance of Lamb waves signals and the wavefield, such as the disk-wrapped electrode induces the non-axisymmetric wavefield [7], signal amplitude variation with a different type of adhesive and PZT thickness effects

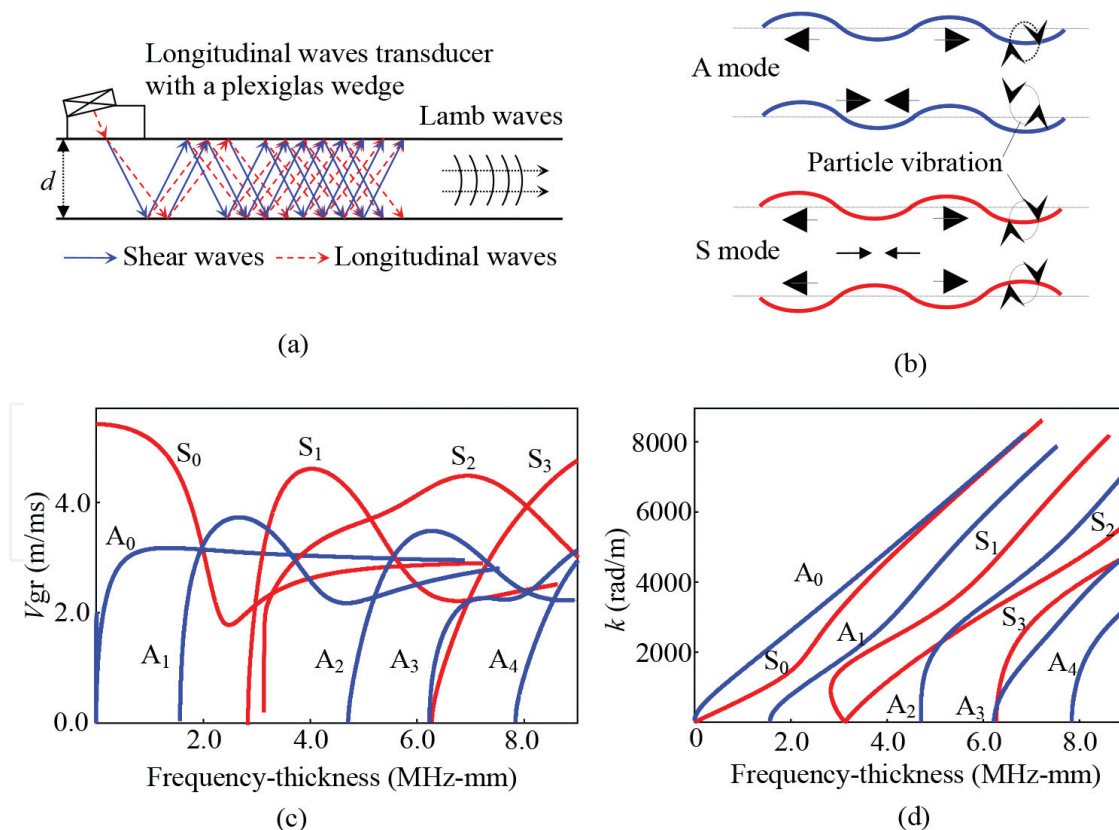


**Figure 1.** Characteristic of Lamb waves in an aluminum plate drawn with DISPERSE. (a) Oblique incidence method for Lamb waves generation; (b) vibration property of Lamb waves; (c) group velocity dispersion curves; (d) wavenumber dispersion curves.

[8], Lamb waves signals emitted with the laser beam and PZT show non-stationary and stationary property, respectively.

3. Material and structure of plates yield the wavefield, such as anisotropic property of composite plates leading the inhomogeneity distribution of wavefield in spatial and temporal dimensions [9, 10], echoes from the edges, stiffeners, bolts and rivets in the complex structure reduce the interpretability of the received Lamb waves signals [11].
4. Environmental and operational condition change the material properties and further influence the emitting, propagation and the sensing of Lamb waves [12, 13], typically the temperature and the local concentrated stress. The temperature changes (a) the plate material stiffness affects the waves phase/group velocity [14, 15]; (b) the dielectric permittivity and piezoelectric coefficient of piezoelectric transducers [16] and (c) the adhesive stiffness and then modifies the transducer-plate bonding shear stress transmission and minor thermal expansion/contraction occurring within the adhesive layer can yield to a slight shift in the peak frequency response [17]. The variation of the loads during usage changes resulting a slight anisotropy of the structure and further induces the velocity directionality [18]. Meanwhile, it also induces the time shifts effect under loads conditions that are of the same order as those caused by temperature change.

As illustrated in the above content, the factors influencing signals features, the environmental and operation condition, Lamb waves, transducers, plate-like structures and the defects are combined and form a close detection/monitoring ecosystem in which the transducers realize the energy conversion between the systems and the structures. Meanwhile the properties of transducers have influence on the detection/monitoring systems setting strategies and the emitting and sensing of Lamb waves. All these have decided that transducers play a very important role in structure integrity evaluation. Signal processing technologies are adopted to optimize and analysis the acquired data and finally realize structure state evaluation. When the received data have relatively high resolution and interpretability, defects imaging techniques and the intelligent recognition techniques are directly applied for structure integrity evaluation; otherwise, the signals should be pre-processed with signal optimization techniques to improve their resolution and interpretability through modulating waveforms, multi-scale analysis and temperature effect compensation. Considering the importance roles of transducers and the signal processing strategies used in Lamb waves based structure integrity evaluation, the structure of this chapter is setting as: Section 2 introduces several kinds of transducers used for Lamb waves emitting and sensing. Then some signal processing technologies for dispersion compensation, time-frequency analysis and overlapping waveform decomposition, and illuminating the influence temperature effects are briefly reviewed in Section 3. Finally, a short summary and conclusions are provided.

## 2. Transducers and specific Lamb wave mode emitting

There are mainly three kinds of transduction mechanism used for the design of the transducers in structure integrity evaluation, including piezoelectric effect, electromagnetic ultrasonic coupling mechanisms and laser thermodynamics. In this section, we will briefly review some



typical transducers and their application for specific mode of Lamb waves emitting and sensing.

## 2.1. Piezoelectric transducers

Piezoelectric materials have piezoelectric effect that can be used to achieve energy conversion between mechanical energy and electrical energy. As shown in **Figure 2(a)**, when the piezoelectric material is loaded with an alternating voltage, it may produce an oscillatory mechanical vibration, and form pressure at its surface or sound waves in the around air. Vice versa, an oscillatory expansion and contraction of the material produce an alternating voltage at the terminal. This phenomenon is named as the piezoelectric effect. The geometry size, polarization direction and the voltage frequency have influence on the vibration mode of the piezoelectric materials. Many kinds of piezoelectric transducers have been designed in laboratories and corporations.

Piezoelectric wafer active transducers (PWATs) have relative simple round or rectangle geometrical shapes. Typically, these transducers have electrodes on the top and bottom surfaces as plotted in **Figure 2(b)**. With the piezoelectric effect, PWATs actuate and sense Lamb waves signals in the structure directly through in-plane strain coupling. More differences between the PWATs and conventional ultrasonic transducers are listed in Ref. [19]. Interdigital transducers (IDTs) have electrodes shaped in a comb pattern that are designed with traditional piezoelectric ceramics or the novel piezoelectric materials, such as macro-fiber composite (MFC) [20] and poly vinylidene fluoride (PVDF) piezoelectric polymer film [21–23]. **Figure 2(c)** plots an interdigital transducer. Through adjusting the space between adjacent interdigital electrodes, IDTs are able to generate Lamb waves with a specific wavelength. Comparing with the piezoelectric ceramics, the novel piezoelectric materials feature better flexibility, higher dimensional stability and more stable piezoelectric coefficients over time. They can be of various shape to cope with curved surfaces for signal sensing in low frequency range due to their weak driving. The tunable IDTs have a series of density distributed discrete electrode stripes that are connected in various configurations [24]. In the application, Lamb waves with different wavelengths can be emitted through adjusting the configuration of the interdigital electrodes. As shown in **Figure 2(d)**, air-coupled ultrasonic transducers [25] are often used for non-contact

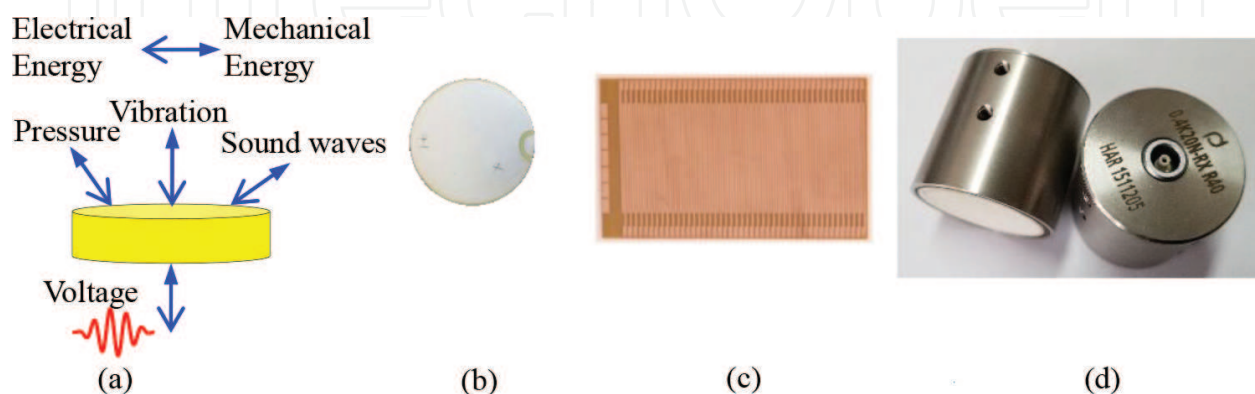


**Figure 2.** Typical piezoelectric effect-based transducers. (a) Piezoelectric effect; (b) PWAT; (c) Interdigital transducer; (d) air-coupled transducers.

and non-contaminating ultrasonic scanning detection. The proportion of the ultrasonic energy transmitted through an interface depends on the acoustic impedance match ratio of the two materials. The higher match ratio, the more energy is transmitted into the plates. Thus, it is important to minimize these losses to obtain an acceptable signal to noise ratio. With the development of micro-electro-mechanical technology, micro-machined ultrasonic transducers are researched [26] that have many advantages over conventional ultrasonic transducers, including miniature size, low power consumption and the ability to create one-dimensional (1D) and two-dimensional (2D) array structures.

The techniques for pure mode emitting and sensing have been studied with the piezoelectric transducers. Theoretical models researches of PWATs [27] show that the displacements at the plate surface is a function of an interelement distance for a specific Lamb waves mode. With the theory, dual-element transducers are placed at a specific distance on the same surface of a plate for pure  $A_0$  mode emitting, or two dual PZTs (concentric disc and ring) structure is adopted to tune the excited signal properly for specific mode emitting, or to decompose both mode contributions in the received signals [28]. The IDTs can realize pure mode emitting by adjusting the interspace between individual electronic elements of the piezoelectric array or adding backing materials to the elements [29]. While the interaction between individual elements may have a significant influence on the performance of the IDTs, these effects cannot be neglected even in the case of low frequency excitation. Researchers deposited symmetrical transducers on both sides of the plate to generate pure Lamb waves mode [30], in which for electric symmetrical connection to the two transducers,  $S_0$  mode is generated, vice versa, for the anti-symmetrical electric connection,  $A_0$  mode is strong and  $S_0$  mode is suppressed. Degertekin et al. [31] added hertzian contacts between the plates and the end of specially designed quartz rods, which guide anti-symmetric modes generated by PZT-5H transducers bonded at their other end. For an angle beam transducer, a low-attenuation Lamb waves mode was generated by setting the incidence angle [32]. Other literatures studied theoretical model of the PWAS-related Lamb waves to identify the single mode emitting frequency, then adopted the post-process technique, such as time reversal, to enhance the mode purity [33, 34]. As the symmetric modes have more energy components in the out-of-plane direction, air-coupled ultrasonic transducer can be very suitable for pure  $A_0$  mode emitting and sensing [35]. The high-order or high frequency-thickness Lamb waves have more complex wave structure and shorter wavelength, while more sensitive to the characteristic change of plates. Higher Order Mode Cluster (HOMC) is proposed by Jayaraman et al. [36], it used the nature that multiple modes concentrate together to form a cluster. Khalili et al. [37] realized single Lamb waves mode emitting at 20 MHz-mm with the HOMC method.

## 2.2. Electromagnetic acoustic transducer

Electromagnetic acoustic transducer (EMAT) consists of permanent magnets, coils and a metal material in which the magnets introduce the static magnetic field. The principle of the electromagnetic ultrasonic coupling mechanisms is shown in **Figure 3(a)**. When the current is loaded on the coils, eddy currents will be generated in the conductive structure and form three kinds of electromagnetic coupling mechanisms for ultrasonic waves emitting and sensing: Lorentz

force, magnetostriction mechanism and magnetizing force. In addition, Lorentz force mechanism exists in all conductive materials, whereas the magnetostriction mechanism only exists in ferromagnetic materials. Compared with the other two mechanisms, the magnetizing force is very weak and is often neglected in studies. Various types of EMAT can be designed by changing the configuration of the permanent magnet and coil to realize easily the attenuation of pure Lamb waves mode. **Figure 3(b)** shows the EMAT with solenoid sensing coils and a cylindrical magnet; **Figure 3(c)** shows the Panametrics E110-SB EMAT developed by OLYMPUS.

By adjusting the spacing of meandered line coils equal to the half wavelength of Lamb waves, EMAT can easily realize Lamb waves emitting and sensing at specific frequency. Meanwhile, researchers have developed many kinds of EMATs through specific design of the geometry and the position of the magnets and coils [38], including omnidirectional  $S_0$  mode EMAT [39], omnidirectional  $A_0$  mode EMAT [40] and directional magnetostrictive patch transducer [41]. While the EMAT is difficult to generate a pure Lamb wave mode when dispersion curves of several modes are close together; however, by narrowing the frequency bandwidth via a large number of cycles in the excitation signal, pure mode generation via an EMAT is shown to be possible even in areas of closely spaced modes [42]. Experimentally, the EMAT can scan along the surface, while the loading voltage is often very high compared with that of piezoelectric transducers. EMATs are also used for high-order Lamb waves emitting and sensing in a 6mm-thick steel plate [43].

### 2.3. Laser ultrasonic systems

Laser ultrasonic systems (LUS) have three basic functional components: a generation laser, a detection laser and a detector. The generation laser emits a laser beam that irritates on the surface of plates to generate ultrasonic waves based on thermoelastic regime or ablation regime. In the thermoplastic regime, the ultrasonic waves are generated from the thermoelastic

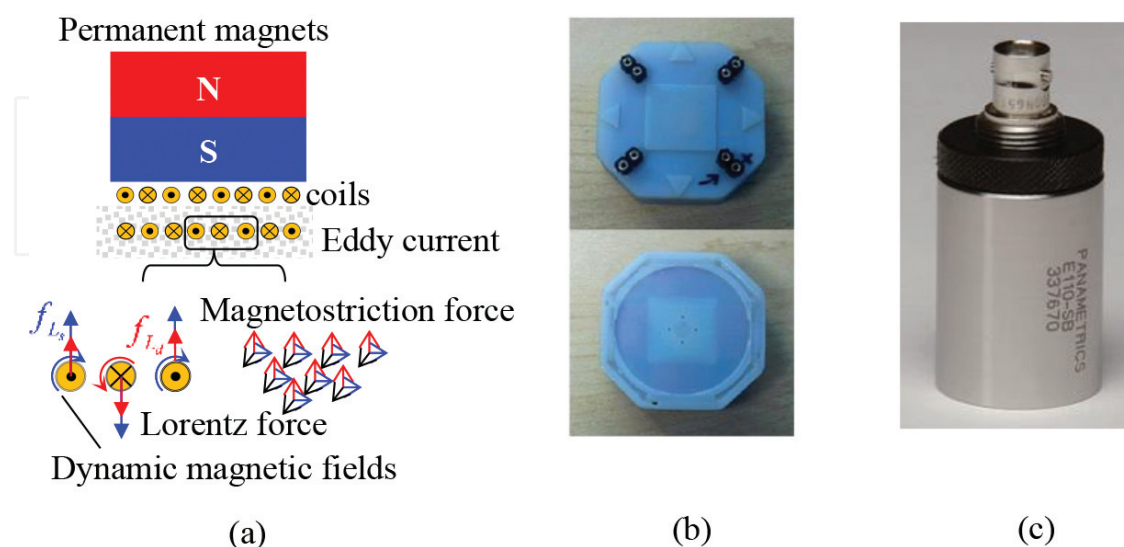


**Figure 3.** Electromagnetic ultrasonic coupling mechanisms transducers. (a) Principle of the electromagnetic ultrasonic coupling mechanism; EMAT with four solenoid sensing coils and a cylindrical magnet [43]; Panametrics E110-SB EMAT.



expansions of materials. While, in the ablation regime, the ultrasonic waves are generated from the material removal that will induce damage to the surface of plates. The laser ultrasonic systems are carefully set to work in the thermoelastic regime in Lamb waves integrity evaluation. Additionally, the laser-generated Lamb waves signal is a broad bandwidth signal in which several Lamb wave modes can be acquired in a single measurement, providing more opportunities to selectively generate the desired modes. **Figure 4(a)** plots the elastic waves generated by laser beam under thermoelastic regime.

The detection laser and detector are used for ultrasonic waves detection based on various principle including Doppler frequency shift, speckle interferogram and Fabry-Pérot detection schemes. A laser vibrometer principle of operation allows for measuring velocity of a point along the axis of laser beam incidence onto the surface based on the Doppler frequency shift principle. In 1997, researchers started sensing the out-of-plane displacements of Lamb waves with an optical fiber Michelson interferometer. The progress in the development of equipment related to scanning laser Doppler vibrometry (SLDV) resulted in the availability of the full wavefield measurements of Lamb waves propagating in metallic specimens. Shearography is an interferometric technique for surface vibration measurement. In a digital shearography system, the inspected object is illuminated by an expanded laser beam, forming a speckle pattern. The speckle patterns are optically processed by a shearing device, and the resultant interferogram is recorded by a charge-coupled device camera. Speckle interferogram, recorded before and after object deformation, are correlated to yield correlation fringes. The phase of these fringes can represent the displacement gradient of the specimen. More detail information about the system is introduced in Ref. [44]. The elastic waves generate a change in the index of refraction of the surface, incident laser beams will deflect slightly and thus change course. This detected change is converted into an electrical signal. **Figure 4(b)** plots the laser ultrasonic principle.

As the laser beam is irradiated on the normal direction of the out-of-plane that is the main displacement components of anti-symmetric modes. In the detection process, people can adjust the shape and the spatial distribution of the laser beams to reduce the energy loss and further form a specific modes wave. Many types optical path adjusting elements are adopted for specific Lamb waves mode emitting, including Fresnel lens, rectangular cylinder lens [45, 46], marks for creating predetermined spatial laser light distributions [47] and periodic spatial array of laser sources [48]. The interference pattern of two high power laser beams on a sample surface produces periodic heating and then generating anti-symmetric Lamb waves [49]. By

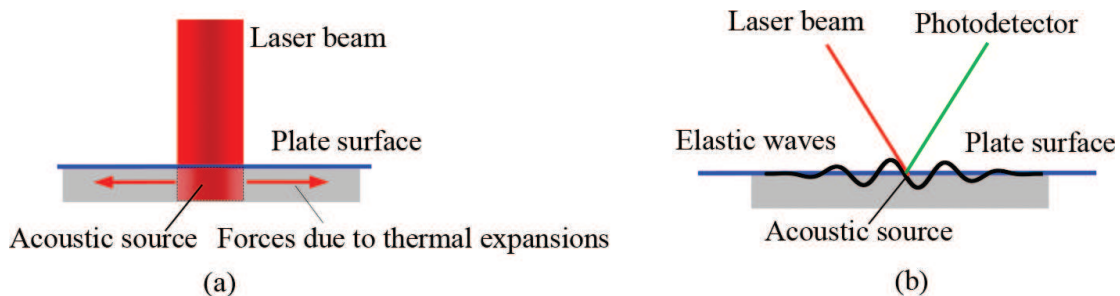


**Figure 4.** Principle and systems for laser ultrasonic inspection. (a) Elastic waves generated by laser beam under thermoelastic regime; (b) laser ultrasonic principle.

varying the interface fringe spacing, the acoustic frequency is easily and continuously tunable from 2.5 to 23 MHz.

Other transducers used in structural integrity evaluation but not just piezoelectric ceramic fibers, fiber optic transducers [50] and microelectronic transducers. Piezoelectric fibers having a metal core can activate Lamb waves in composite plates transverse to the fibers with radial displacement components originating from the  $d_{33}$  coupling coefficient. They can also generate Lamb waves in the direction of the piezoelectric fibers using the  $d_{31}$  coupling coefficient. The fiber optic transducers are used for Lamb wave sensing, through connecting a fiber Bragg gratings (FBG) filter with a photodetector, the light intensity induced by the Lamb waves, rather than strain itself, can be sensed at a high sampling rate. The FBG has strong directivity in sensing Lamb wave signals.

### 3. Signal optimization techniques

The signal processing techniques for improving the resolution and the interpretability of Lamb wave signals are termed as the signal optimization techniques in this section. There are waveform modulation techniques such as multi-scale analysis techniques and temperature effect compensation techniques. These techniques are adopted for Lamb waves dispersion compensation, high-resolution signal emitting and sensing, overlapping waveforms decomposition, time-frequency analysis and temperature effect compensation.

#### 3.1. Waveform modulation techniques

When an excitation signal,  $f(t)$ , is emitted into a plate at original position, the received signal,  $u(x, t)$ , at  $x$  position can be expressed as

$$u(x, t) = \frac{1}{2\pi} \int_{-\infty}^{\infty} F(\omega) e^{j(\omega t - kx)} d\omega, \quad (4)$$

where  $F(\omega)$  is the Fourier transform of the excitation signal and  $k$  is the angular wavenumber. In Eq. (4), there are several parameters that decide the signal resolution and interpretability, including the amplitude, phase and frequency variation with the duration. The signal processing techniques process through modulating these fundamental signal parameters for adjusting the signal waveforms are termed waveform modulation techniques that are used for Lamb waves dispersion compensation, high-resolution Lamb waves detection and defects information extraction in structural integrity evaluation.

Signal processing techniques for dispersion compensation are realized through modulating the frequency or the wavenumbers of the received Lamb waves signals, because the dispersion nature of Lamb waves is shown as the nonlinear characteristic of signal phase in mathematical form. Time recompression technique [51] compensates the dispersion using spatial phase shift arising at each signal frequency component from the propagation of the waves over a large distance. The back-propagation function in the technique can only provide the first-order phase shift. Time-distance mapping technique [52] compresses dispersive signals by converting the

signals in frequency domain to a specific propagation distance by back-propagating signals to  $t = 0$  using the known dispersion relation. Considering the relationship between the angle frequency  $\omega$  and the wavenumber, backward Lamb waves of Eq. (4) at  $x$  can be expressed as

$$u_b(-x) = \frac{1}{2\pi} \int_{-\infty}^{\infty} U(\omega) e^{jkx} d\omega = \frac{1}{2\pi} \int_{-\infty}^{\infty} U(\omega) c_g(\omega) e^{jkx} dk, \quad (5)$$

where  $\omega_0$  is the specific frequency and  $U(\omega)$  is the Fourier transform of the original received signal,  $u(x, t)$ .

Beside interpolating  $G(\omega)$  and  $c_g(\omega)$ , the variables in spatial-wavenumber domains in time-frequency domains are needed to ensure the calculation accuracy. Spectral warping technique [53–55] was applied for the removal of dispersion from a signal in time-space domain using frequency transformation. The rescaling is defined mathematically by a composition of the signal spectrum with a function closely related to the dispersion relation that is independent of propagation distances and can be applied to signals consisting of multiple arrivals with the same dispersion characteristics. The wideband dispersion reversal technique [56], as expressed in Eq. (6), makes use of a priori knowledge of the dispersion characteristics to synthesize the corresponding dispersion reversal excitations, which is able to selectively excite the self-compensation pure mode waveforms.

$$\begin{aligned} \text{WDR}[u(\tau_0 - t)] &= \frac{1}{2\pi} \int_{-\infty}^{+\infty} U(-\omega) e^{-j\omega\tau_0} \cdot H'(\omega) e^{j\omega t} d\omega \\ &= \frac{1}{2\pi} \int_{-\infty}^{+\infty} F(-\omega) \cdot H'(-\omega) \cdot H'(\omega) e^{j\omega(t-\tau_0)} d\omega \\ &= \frac{1}{2\pi} \int_{-\infty}^{+\infty} F(-\omega) e^{j\omega(t-\tau_0)} d\omega \\ &= f(\tau_0 - t), \end{aligned} \quad (6)$$

The above-mentioned algorithms are limited in practical application as the propagation distance may be unknown. Wavenumber curves linearization technique [57, 58] uses the first- or second-order Taylor expansion to linearize the nonlinear wavenumber. It is independent on the propagation distance and can be applied to the signals constructed with multiple arrivals with the same wave mode or dispersion characteristics. It has less computation efforts than the time-distance mapping technique. With the idea of nonlinear wavenumber linearization, Cai et al. [59] extended the wavenumber linearization technique and developed the linearly dispersive signal construction and non-dispersive signal construction method these are expressed as

$$\begin{aligned} u_{\text{lin}}(t) &= \frac{1}{2\pi} \int_{-\infty}^{\infty} M(\omega - \omega_c) e^{-i[k_0 + k_1(\omega - \omega_c)]x + i\omega t} d\omega \\ &= \frac{e^{i\omega_c t - ik_0 x}}{2\pi} \int_{-\infty}^{+\infty} M(\omega) e^{-i\omega k_1 x + i\omega t} d\omega \\ &= m(t - k_1 x) e^{i\omega_c t - ik_0 x} \\ &= f(t - k_1 x) e^{i(k_1 \omega_c - k_0)x}, \end{aligned} \quad (7)$$

where  $\tau_0$  is a time delay constant,  $M(\omega - \omega_c) = u(\omega)$  is the Fourier transform result of the amplitude modulation function with shift  $\omega_c$ ,  $\omega_c$  is the center frequency of the excitation,

$k_0 = \omega_c/c_p(\omega_c)$ ,  $k_1 = dk_0/d\omega|_{\omega=\omega_c} = 1/c_g(\omega_c)$ ,  $H(-\omega) = e^{-ik(-\omega)x}$  is the phase spectrum of the dispersion function and  $K_0(\omega)$  is the wavenumber that determines the dispersion relation of Lamb waves mode. The above-mentioned techniques are performed with the received Lamb waves signals that can be named as the post-processing dispersion compensation techniques and more detail process of them are introduced in Refs [51–53, 57–60].

The other signal processing strategy for high-resolution detection is realized through modulating the waveform of excitation signals, termed the excitation modulation techniques, in which the excitations are built based on the dispersion characteristics of Lamb waves, the propagation distance and the travel time [61] or utilize the chirp technique to established effects on the original excitation signal for a given compensation distance, and thus the response extraction and the dispersion compensation can be made simultaneously [62]. For pulse compression (PuC) techniques, a  $\delta$ -like wave packet can be generated with a broader auto-correlation of a specific waveform including linear chirp signal, nonlinear chirp signal, Barker code and Golay complementary code. The linear chirp has the smallest main lobe width, corresponding to the best inspection resolution; the nonlinear chirp and Golay complementary code are with smaller sidelobe level, corresponding to the better performance in terms of side lobe cancelation [63], and the waveform comparisons are still effective with small errors in dispersion compensation. Malo et al. [64] presented a 2D compressed analysis, which combines pulse compression and dispersion compensation techniques in order to improve the SNR, temporal-spatial resolution and extract accurate time of arrival of responses. Yücel et al. [65] utilizes maximal length sequence (MLS) signals to produce a brute-force search-based dispersion compensation and cross-correlation for defects location. Compared with a linear broadband chirp, the technique using MLS combined with cross-correlation can improve SNR and facilitate the accurate extraction of time-of-flight (ToF), even in complex multimode situation. Marchi et al. [66] proposed a code division strategy based on the warped frequency transform. In the first, the proposed procedure encodes actuation pulses using Gold sequences. Then for each considered actuator, the acquired signals are compensated from dispersion by cross-correlating the warped version of the actuated and received signals. Compensated signals from the base for a final wavenumber imaging meant at emphasizing defects and/or anomalies by removing incident wavefield and edge reflections. Hua et al. [67] proposed pulse energy evolution method for high-resolution Lamb wave inspection. Some conclusions were obtained as follows. Linear chirp signal combined with pulse compression provides a  $\delta$ -like excitation with a high signal-to-noise ratio. By the application of dispersion compensation with systemically varied compensation distances, an evolution of compensation degree curve can be obtained to estimate the actual propagation distance of the interested wave packet.

Time reversal (TR) technique can focus the elastic waves to its original shape by time-domain reversal of the received signal with the reciprocity principle. **Figure 5** shows the principle diagram of time reversal technique that consists of the forward propagation and backward propagation. In the forward propagation, a signal,  $f(t)$ , is emitted into the plate by the transducer A, and received by transducer B. Then received signal is reversed in time domain and reemitted by the transducer A in the backward propagation process. The final TR processed result is received signal at transducer B. To avoid the inconvenience in the process of classical time reversal, a pure numerical signal process technique for TR technique is developed, termed the virtual time reversal technique, and can be expressed as



$$f_{\text{TR}}(t) = \text{ifft} \left\{ \text{fft}[u(-t)] \frac{\text{fft}[u(t)]}{\text{fft}[f(t)]} \right\}, \quad (8)$$

where  $f(t)$  is the excitation signal,  $u(t)$  is the original received Lamb waves signal,  $u(-t)$  is the time reversal result of signal of  $u(t)$ ,  $f_{\text{TR}}(t)$  is the time reversal result, fft and ifft are the fast Fourier transform and its inverse transform.

It has been studied for dispersed compression [60, 68] and defects information extraction [69, 70]. Zeng et al. [70] carefully designed the amplitude of the input signal before the time reversal process. Huang et al. [71] used a weight vector to modulated the signal in both the forward and backward processes, the vector is obtained as the product of the reciprocal of amplitude dispersion and a window function that varies with the excitation signal adaptively, and its shape is also determined by a threshold. The advantages of single mode tuning in the application of time reversal damage detection are highlighted in Refs. [33,71]. The adhesive, host plate, transducer and excitation parameters are also influenced on the performance of time reversibility of Lamb waves.

### 3.2. Multi-scale analysis techniques

Multi-scale analysis techniques map a 1D signal into a high dimensional space with transform based on a kernel function, including short-time Fourier transform (STFT), Wavelet transform (the continue wavelet transform (CWT), the discrete wavelet transform (DWT) and wave packet transform), Gabor transform [72], Chirplet transform [73] and asymmetric Gaussian Chirplet transform [74, 75]. When the mapping data space express the changing frequency of the signal parameters, the algorithm can be used for time-frequency analysis [76]. In other case, the mapping data space indicates the inner product between the signal and a kernel function, the algorithm can be used for Lamb waves mode identification and overlapping waveforms decomposition. The formula of STFT and CWT can be expressed as Eq. (9) and Eq. (10), respectively.

$$y(\omega, \tau) = \int_{-\infty}^{+\infty} u(t)w(t - \tau)e^{-j\omega t}dt, \quad (9)$$

$$y(s, \tau) = \frac{1}{\sqrt{s}} \int_{-\infty}^{+\infty} u(t)\psi^*\left(\frac{t - \tau}{s}\right)dt, \quad (10)$$

where  $w(t)$  is the window function, commonly a rectangle window, Hanning window or Gaussian window;  $u(t)$  is the sensing Lamb waves signal,  $\psi$  is the mother wavelet,  $\tau$  is the shift step in time-axis,  $s$  is the scale and \* indicates the complex conjugate operation.

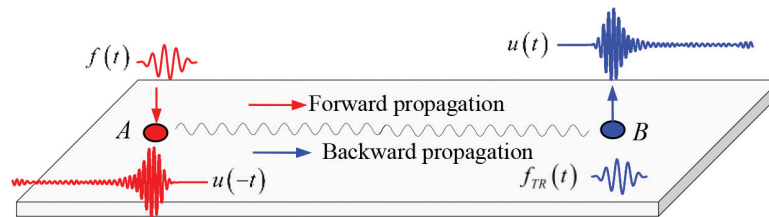


Figure 5. Principle diagram of time reversal technique.



STFT divides a signal into blocks with fixed window width that controls the trade-off of bias and variance. Shorter window leads to poor frequency resolution, while longer window improves the frequency resolution but compromises the stationary assumption within the window. Thus researchers adopted variable window width instead of constant-width [77, 78] into the STFT to deal with the local resolution requirement. CWT projects a signal into a class of kernel function, termed mother wavelet, that usage of scale factor that is inversely proportional to the frequency of the given signal. Limited by the Heisenberg uncertainty principle that can be briefly described as the time-frequency windows have constant area, its results have higher frequency resolution and lower time resolution for lower frequency components, while have lower frequency resolution and higher time resolution for higher frequency components. Meanwhile the frequency resolution at the same scale level cannot be adaptively adjusted. The time-frequency representation concentration cannot be significantly improved for non-stationary signal with rapidly time-varying frequency component with the STFT and CWT. Reassignment method is a post-processing technique putting forwards to improve the readability of time-frequency representation. Through assigning the average of energy in a domain to the gravity center of these energy contributions, the reassignment technology reduces energy spread of time-frequency representation at the cost of greater computational complexity. However, it is sensitive to the noise, and inevitably introduces interference terms since the computed gravity center unnecessarily represents the real energy distribution of the interested signal. Wigner-Ville distribution (WVD) is a representative of bilinear time-frequency analysis in which the process is based on the Fourier transform of instantaneous auto-correlation function of the signal. WVD could generate time-frequency representation with the high concentration, while it also introduces plenty of cross-terms. Hilbert-Huang transform uses empirical mode decomposition (EMD) to decompose a signal into several intrinsic mode functions (IMF) along with a trend and obtain instantaneous frequency [79]. EMD is a data-driven signal decomposition technique that sequentially extracts zero-mean regular/distorted harmonics from a signal, starting from high- to low- frequency components, and it is a dyadic filter equivalent to an adaptive wavelet. While the end effects influence the performance of the signal decomposition and distort the results. For this case, researchers proposed various signal extension technique to solve the problem of end effects, including feature-based extension, mirror images, prediction methods and pattern comparison [80].

The general formula of Gabor transform, Chirplet transform and asymmetric Gaussian Chirplet transform can be expressed as Eqs. (11) and (12). Their results are the inner product between the signal  $u(t)$  and the complex conjugate of kernel function  $g_{\tau,\omega,\Theta}$ .

$$y(\tau, \omega; \Theta) = \int_{-\infty}^{+\infty} u(t) g_{\tau,\omega,\Theta}^*(t) dt, \quad (11)$$

$$g(t) = \begin{cases} e^{-\pi(\frac{t-\tau}{s})^2} \cos [\omega(t-\tau) + \phi], & \text{Gabor} \\ (\sqrt{2\pi}s)^{-1/2} e^{-\pi(\frac{t-\tau}{s})^2} \cos [\omega(t-\tau) + \zeta(t-\tau)^2 + \phi], & \text{Gaussian Chirplet} \\ ae^{-\alpha(1-r \tanh(\kappa(t-\tau)))(t-\tau)^2} \cos [\omega(t-\tau) + \zeta(t-\tau)^2 + \phi], & \text{asymmetric Gaussian Chirplet,} \end{cases} \quad (12)$$

where  $\zeta$  is the linear chirp rate,  $\phi$  is the phase,  $a$  is the amplitude,  $\alpha$  is the decay rate controlling the signal bandwidth,  $r$  is the asymmetry factor controlling the skewness of the window and  $\tanh(\kappa t)$  is hyperbolic tangent function of order  $\kappa$ , a positive constant integer. The detail description of Eq. (11) is given in Refs [81, 82]. Gabor transform and the Chirplet transform projects a signal energy distribution in a time-frequency plane, which does not induce interference terms [83]. An important advantage of such analysis is to provide highly concentrated time-frequency representation with signal-dependent resolution. Especially for the latter one, there are many parameters adaptively adjusted for an accuracy mapping the signal features, including the center frequency, arrival time, duration and frequency-varying characteristics. These two algorithms can also be used for decomposition of the overlapping waveforms.

The signal decomposition is based on a reasonable assumption that a signal can be expressed as a sum of several wave packets, as shown in Eq. (14).

$$u(t) = \sum_{n=0}^{N-1} \langle R^n u, g_{\gamma_n} \rangle g_{\gamma_n} + R^N u, \quad (13)$$

where  $u(x, t)$  is the signal received at  $x$  that contains the first arrival waves, the echoes from the edges of plates and the defects;  $R^N u$  is the residual term;  $N$  is the number of iterations;  $g_{\gamma_n}$  is the matching atoms that fit to the residual term  $R^n u$ , which is the residual left after subtracting results of previous iterations;  $g_{\gamma_i}$  is the atoms in a pre-built over-complete dictionary or a sub-type of a kernel function. The derivation processes of parameters  $R^n u$  and  $g_{\gamma_n}$  can be expressed as

$$\begin{cases} R^0 u = u(t) \\ R^{n+1} u = R^N u - \langle R^n u, g_{\gamma_n} \rangle g_{\gamma_n} . \\ g_{\gamma_n} = \arg \max_{g_{\gamma_i} \in D} |\langle R^n u, g_{\gamma_i} \rangle| \end{cases} \quad (14)$$

In the process of the wave packets decomposition, the atoms can be selected from a pre-built dictionary or sub-type of a kernel function. The dictionary can be built based on the pre-analysis of the excitation [84], the interaction between Lamb waves and defects [85], etc. Mallat et al. [86] introduced the matching pursuit with time-frequency dictionaries. The decomposition based the Gabor transform and the Gaussian Chirplet transform are suitable for the signals with symmetric envelopes, while the sensing signals often have asymmetric envelopes induced by the dispersion nature of Lamb waves. Thus, the asymmetric Gaussian Chirplet is designed for decomposition the dispersive Lamb waves signal benefiting from its specific designed windows.

Matching pursuit algorithm is a highly adaptive signal decomposition and approximation method for de-noising, wave parameter estimation and feature extraction [86, 87], while it does not provide the best approximation to signal by a linear combination of atoms from a dictionary or a sub-type of kernel function. Actually, many parameters need to be estimated in each iteration step to get a best approximant, it is an NP-hard problem. Therefore, a suitable parameter evaluation algorithm is very important for signal decomposition algorithms. The successive parameters estimation algorithm [88] and the fast ridge pursuit algorithm [82] are most used algorithms for estimation of the atom parameter. In each iteration of the pursuit, the

best atom is first selected, and then, its scale and the chirp rate are locally optimized so as to get a 'good' chirp atom. While the successive parameter estimation is a suboptimal method. The error in one parameter estimate due to noise will induce errors in estimation of other parameters. Zeng et al. [89] combined the adaptive Chirplet transform and the time-varying band-pass filtering provides a methodology for extracting interest waveforms from the overall Lamb wave signals.

### 3.3. Temperature effect compensation techniques

The signals received under a vibration of temperature condition can be expressed as [90, 91].

$$u(t; T_0 + \delta T) = \sum_{j=1}^N a_j s_j [t - t_j \beta(\delta T)], \quad (15)$$

where  $a_j$ ,  $s_j$  and  $t_j$  are the amplitude, the waveform and the arrival time of the  $j^{\text{th}}$  wave packet respectively,  $\beta(\delta T)$  is the shift in arrival times of wave packets in each time-trace with respect to their values at an arbitrary fixed temperature,  $\beta = 1 - \delta T \cdot c_g k_p / c_p^2$ ,  $k_p$  is the change in phase velocity with temperature.

The optimal baseline selection (OBS) and the baseline signal stretch (BSS) are widely studied [92] for elimination the temperature effect in Lamb waves based structure integrity evaluation. In OBS technique, a pre-built database under different temperatures is built. The process for OBS includes (1) recording a set of baseline waveforms from the intact specimen at temperatures spanning the expected operating range; (2) selecting a waveform from the baseline set, which the temperature is the closest to the measured signal; (3) adjusting the baseline waveform to best match the signal, then calculating an error parameter between the signal and the adjusting waveform and (4) comparing these parameters with a threshold to determine the structural status. A large number of baselines data are needed even for small temperature steps to ensure the accuracy of the extracted defects waveforms that increase computational and memory costs. Meanwhile the damage manifests itself and the noise will rise the OBS error [93]. Wang et al. [94] combined the OBS and the adaptive filter to compensate the temperature variations. The simplistic representation of the signal and the choice of activation function are the main limitations of this technology. BSS modified a single baseline time-trace to match the field time-trace to compensate the temperature effect. In BSS, the time-axis of the baseline time-trace is stretched by a stretch factor to yield a new time-trace, while the BBS is strongly dependent on the mode purity and structural complexity. The OBS and the BBS can be combined to form a robust temperature compensation strategy [90, 95]. The reduction in the number of baselines in the database is limited by the maximum temperature gap between baselines, which can be compensated for by the optimal stretch without loss of sensitivity; this is a function of mode purity, signal complexity and the maximum propagation distance to cover the whole structure expressed in wavelengths [96]. Their formula are

$$u_m(t; T_m) = \sum_{j=1}^N a_j^m s_j^m [t - t_j^m \beta(\delta T_m)], \quad (\text{OBS}) \quad (16)$$

$$\hat{u}(t; T_0, \hat{\beta}) = u(t/\hat{\beta}; T_0) = \sum_{j=1}^N a_j s_j(t/\hat{\beta} - t_j), \quad (\text{BSS}) \quad (17)$$

where  $u_m$  is the  $m^{\text{th}}$  time-trace from the baseline dataset,  $T_m = T_0 + \delta T_m$  refers to as the baseline dataset and  $\beta(\delta T_m)$  is the fractional shift in arrival times of wave packets in each time-trace with respect to their values at an arbitrary fixed temperature.  $\hat{\beta}$  is a stretch factor to yield a new time-trace  $\hat{u}(t; T_0, \hat{\beta})$ .

Other techniques have been proposed for compensation the temperature effect. Physics-based approach builds the compensation data through analyzing the temperature effect on the structures and transducers [97]. This approach needs to train with prior data, which are always unavailable. Fendzi et al. [98] presented a data-driven temperature compensation approach, which considers a representation of the piezo-sensor signal through its Hilbert transform that allows one to extract the amplitude factor and the phase shift in signals, while its compensation accuracy depends on the length of the time window that should be considered in the temperature compensation parameters estimation. Liu et al. [99] proposed a baseline signal reconstruction technique in which the Hilbert transform is used to compensate the phase of baseline signals and the orthogonal matching pursuit is used to compensate the amplitude of baseline signal. Dao et al. [100] combined the cointegration technique and fractal signal processing to effective removal of undesired multiple temperature trends in Lamb waves signals. The former technique relies on the analysis of non-stationary behavior, whereas the latter brings the concept of multi-resolution wavelet decomposition of time series. While the self-similar pattern of cointegration residuals will be broken when damage is present.

## 4. Summary and conclusions

Lamb waves are a type of elastic waves propagating in plate-like structures that have been widely studied for defects location, sizing and recognition during the past decades. The detection or monitoring system settings, the transducers, the nature of Lamb waves, the environment and operational condition are three key factors influence Lamb waves emitting and sensing, and further decide the design and the performance of signal processing techniques. Considering the important roles of transducers and the signal processing techniques in Lamb waves based structure integrity evaluation, various transducers and signal processing technologies are proposed and developed, and that are briefly reviewed in this chapter.

1. The transducers for Lamb waves emitting and sensing in structure integrity evaluation are mainly based on three types of transduce mechanisms, including piezoelectric effect, electromagnetic acoustic transducer mechanism and laser ultrasonic technique. Piezoelectric transducers, EMAT and laser ultrasonic systems are mostly used for Lamb waves emitting and sensing in structure integrity evaluation. The PWAT, IDTs, the air-coupled transducers are designed with the piezoelectric materials that has high energy conversion efficiency. EMATs are working under electromagnetic acoustic transducer mechanism,



including Lorentz force, magnetostriction mechanism and magnetizing force. Through adjusting the configuration of the permanent magnets, coils, EMATs can be used for relatively pure Lamb wave modes emitting and sensing at specific frequency, including the A modes, S modes. Laser ultrasonic systems commonly consist of a laser transmitter, a laser receiver and a laser demodulator and are very complex systems that are designed with the shearography and the laser vibrometer techniques. In the structure integrity evaluation, the system works under the thermoelastic regime, not the ablation regime, for emitting Lamb waves without the hurt of structure. Through scanning the surface of the plates, the full wavefield Lamb waves can be acquired with the laser ultrasonic system.

2. The waveform modulation techniques, multi-scale analysis techniques and temperature effect compensation techniques are developed to optimize the resolution and interpretability of received Lamb wave signals. Among them, the waveform modulation techniques are used to acquire signals that have more regular waveforms through modulating the phase parameters or the excitation waveforms based on the Lamb wave dispersion principle and the  $\delta$ -like waveform response of specific waves. After the process, the ToF and the scatterers echoes can be analyzed easily. During the process of the time recompression technique, the time-distance mapping technique, the spectral warping technique and the wideband dispersion reversal technique, the propagation should be known that limits their application potentials. The nonlinear wavenumber linearization technique can realize dispersion compensation without the propagation distance parameter. Pulse compression technique also attracts many attentions for generating that highly improve the resolution of the received signals, but it still exists many challenges for field application. TR technique is built with the acoustic reciprocity principle for dispersion compensation and damage feature extraction and is easily realized in applications, while it often cannot get ideal dispersion compensation results. It is more suitable for defects feature extraction in Lamb wave defects detection.
3. Multi-scale analysis techniques are performed through mapping a signal into a multi-parameters data space with a function transform or matching pursuit operation. The transforms based on a kernel function include STFT, CWT, DWT, Gabor transform, Chirplet transform and asymmetric Gaussian Chirplet transform that have been used for time-frequency analysis and overlapping wave packets decomposition. Among them, the wavelet transforms and the Chirplet-based transforms are more attractive as their flexible and more parameter adjusting probability in signal processing. Particularly for the asymmetric Gaussian Chirplet transform has the ability for accurately decomposing the signals with the dispersion characteristics. The dictionary based on overlapping waveforms decomposition techniques is also very attractive. The OBS, the BBS and physics-based approaches are proposed for compensating the temperature effect. OBS is performed with a pre-built database under different temperatures where large number of baseline data are acquired under various temperature conditions. In BSS, the time-axis of the baseline time-trace is stretched by a stretch factor to yield a new time-trace, but it is sensitive to the resolution and the interpretability of Lamb wave signals. The combination of the OBS and BSS can effectively eliminate the shortage in both of the algorithms and have a robust performance in temperature effect compensation. Physics-based approach realizes the



compensation through analysis the temperature effect on the structures and the transducers that is time consuming for field application.

## Acknowledgements

This work was supported by the National Natural Science Foundation of China (Grant Nos. 51475012, 11772014, 11527801, and 11272021).

## Conflict of interest

We declare that we do not have any commercial or associative interest that represents a conflict of interest in connection with the work submitted.

## Author details

Zenghua Liu\* and Honglei Chen

\*Address all correspondence to: liuzenghua@bjut.edu.cn

College of Mechanical Engineering and Applied Electronics Technology, Beijing University of Technology, Beijing, China

## References

- [1] Joseph RL. Guided wave nuances for ultrasonic nondestructive evaluation. *IEEE Transactions on Ultrasonics, Ferroelectrics, and Frequency Control*. 2000;**47**:575-583. DOI: 10.1109/58.842044
- [2] Su ZQ, Ye L, Lu Y. Identification of damage using Lamb waves. *Journal of Sound and Vibration*. 2006;**295**:753-780. DOI: 10.1007/978-1-84882-784-4
- [3] Willberg C, Ducek S, Vivar-Perez JM, Ahmad ZAB. Simulation methods for guided wave-based structural health monitoring: A review. *Applied Mechanics Reviews*. 2015; **67**:1-20. DOI: 10.1115/1.4029539
- [4] Joseph RL. *Ultrasonic Guided Waves in Solid Media*. 2nd ed. New York: Cambridge University Press; 2014. pp. 76-106. ch6
- [5] Giurgiutiu V. *Structural Health Monitoring with Piezoelectric Wafer Active Sensors- Predictive Modeling and Simulation*. 2nd ed. New York: Elsevier; 2014. pp. 293-355. DOI: 10.1016/B978-0-12-418691-0.00020-4.ch6

- [6] Worden K. Rayleigh and Lamb waves-basic principles. *Strain*. 2001;**37**:167-172. DOI: 10.1111/j.1475-1305.2001.tb01254.x
- [7] Moll J, Golub MV, Glushkov E, Glushkova N, Fritzen CP. Non-axisymmetric Lamb wave excitation by piezoelectric wafer active sensors. *Sensors and Actuators, A: Physical*. 2012; **174**:173-180. DOI: 10.1016/j.sna.2011.11.008
- [8] Ha S, Lonkar K, Mittal A, Chang FK. Adhesive layer effects on PZT-induced Lamb waves at elevated temperatures. *Structural Health Monitoring*. 2010;**9**:247-256. DOI: 10.1177/1475921710365267
- [9] Bratton RL, Datta SK, Shah AH. Anisotropy effects on Lamb waves in composite plates. In: *Proceedings of the Review of Progress in Quantitative Nondestructive Evaluation*. Berlin: Springer; 1989. pp. 197-204
- [10] He CF, Liu HY, Liu ZH, Wu B. The propagation of coupled Lamb waves in multilayered arbitrary anisotropic composite laminates. *Journal of Sound and Vibration*. 2013;**332**: 7243-7256. DOI: 10.1016/j.jsv.2013.08.035
- [11] Wang L, Yuan FG. Group velocity and characteristic wave curves of Lamb waves in composites: Modeling and experiments. *Composites Science and Technology*. 2007;**67**: 1370-1384. DOI: 10.1016/j.compscitech.2006.09.023
- [12] di Scalea FL, Salamone S. Temperature effects in ultrasonic Lamb wave structural health monitoring systems. *The Journal of the Acoustical Society of America*. 2008;**124**:161-174. DOI: 10.1121/1.2932071
- [13] Pei N, Bond LJ. Comparison of acoustoelastic Lamb wave propagation in stressed plates for different measurement orientations. *The Journal of the Acoustical Society of America*. 2017;**142**:327-331. DOI: 10.1121/1.5004388
- [14] Putkis O, Dalton RP, Croxford AJ. The influence of temperature variations on ultrasonic guided waves in anisotropic CFRP plates. *Ultrasonics*. 2015;**60**:109-116. DOI: 10.1016/j.ultras.2015.03.003
- [15] di Scalea FL, Matt H, Bartoli I. The response of rectangular piezoelectric sensors to Rayleigh and lamb ultrasonic waves. *The Journal of the Acoustical Society of America*. 2007;**121**:175-187. DOI: 10.1121/1.2400668
- [16] Marzani A, Salamone S. Numerical prediction and experimental verification of temperature effect on plate waves generated and received by piezoceramic sensors. *Mechanical Systems and Signal Processing*. 2012;**30**:204-217. DOI: 10.1016/j.ymssp.2011.11.003
- [17] Sirohi J, Chopra I. Fundamental understanding of piezoelectric strain sensors. *Journal of Intelligent Material Systems and Structures*. 2000;**11**:246-257. DOI: 10.1106/8BFB-GC8P-XQ47-YCQ0
- [18] Lee SJ, Gandhi N, Michaels JE, Michaels TE. Comparison of the effects of applied loads and temperature variations on guided wave propagation. In: *Proceedings of the 37th*

- Annual Review of Progress in Quantitative Nondestructive Evaluation, 18–23 June 2011; San Diego. Huntington Quadrangle: Amer Inst Physics; 2010. pp. 175-182
- [19] Giurgiutiu V. Tuned Lamb wave excitation and detection with piezoelectric wafer active sensors for structural health monitoring. *Journal of Intelligent Material Systems and Structures*. 2005;**16**:291-305. DOI: 10.1177/1045389X05050106
  - [20] Manka M, Rosiek M, Martowicz A, Stepinski T, Uhl T. Lamb wave transducers made of piezoelectric macro-fiber composite. *Structural Control and Health Monitoring*. 2013;**20**: 1138-1158. DOI: 10.1002/stc.1523
  - [21] Mamishev AV, Sundara-rajn K, Yang F, Du YQ, Zahn M. Interdigital sensors and transducers. *Proceedings of the IEEE*. 2004;**92**:808-844. DOI: 10.1109/JPROC.2004.826603
  - [22] Monkhouse RSC, Wilcox PD, Cawley P. Flexible interdigital PVDF transducers for the generation of Lamb waves in structures. *Ultrasonics*. 1997;**35**:489-498. DOI: 10.1016/S0041-624X(97)00070-X
  - [23] Stepinski T, Mańka M, Martowicz A. Interdigital Lamb wave transducers for applications in structural health monitoring. *NDT and E International*. 2017;**86**:199-210. DOI: 10.1016/j.ndteint.2016.10.007
  - [24] Mańka M, Rosiek M, Martowicz A, Stepinski T, Uhl T. PZT based tunable interdigital transducer for Lamb waves based NDT and SHM. *Mechanical Systems and Signal Processing*. 2016;**78**:71-83. DOI: 10.1016/j.ymssp.2015.12.013
  - [25] Castaings M, Hosten B. The use of electrostatic, ultrasonic, air-coupled transducers to generate and receive Lamb waves in anisotropic, viscoelastic plates. *Ultrasonics*. 1998;**36**: 361-365. DOI: 10.1016/S0041-624X(97)00144-3
  - [26] Kusano Y, Wang Q, Luo GL, Lu YP, Rudy RQ, Polcawich RG, Horsley DA. Effects of DC bias tuning on air-coupled PZT piezoelectric micromachined ultrasonic transducers. *Journal of Microelectromechanical Systems*. DOI: 10.1109/JMEMS.2018.2797684
  - [27] Grondel S, Paget C, Delebarre C, Assaad J, Levin K. Design of optimal configuration for generating  $A_0$  Lamb mode in a composite plate using piezoceramic transducers. *The Journal of the Acoustical Society of America*. 2002;**112**:84-90. DOI: 10.1121/1.1481062
  - [28] Emmanuel L, Charles H, Marc R, Nazih M, Christian B. Numerical and experimental study of first symmetric and antisymmetric Lamb wave modes generated and received by dual-PZTs in a composite plate. In: *Proceeding of the Eleventh International Workshop on Structural Health Monitoring*; 12–14 September 2017, California. Pennsylvania: DEStech Publications, Inc.; 2017
  - [29] Liu T, Veidt M, Kitipornchai S. Single mode Lamb waves in composite laminated plates generated by piezoelectric transducers. *Composite Structures*. 2002;**58**:381-396. DOI: 10.1016/S0263-8223(02)00191-5
  - [30] Mao Y, Shui Y, Jiang W, Yin J. Switchable single mode Lamb wave transduction by means of both side excitation. In: *Proceedings of 1995 IEEE Ultrasonics Symposium*; 07–10 November, Seattle. New York: IEEE; 1995. pp. 807-810

- [31] Degertekin FL, KhuriYakub BT. Single mode Lamb wave excitation in thin plates by Hertzian contacts. *Applied Physics Letters*. 1996;**69**:146-148. DOI: 10.1063/1.116902
- [32] Birgani PT, Sodagar S, Shishesaz M. Generation of low-attenuation Lamb wave modes in three-layer adhesive joints. *International Journal of Acoustics and Vibrations*. 2017;**22**: 51-57. DOI: 10.20855/ijav.2017.22.1450
- [33] Xu BL, Giurgiutiu V. Single mode tuning effects on Lamb wave time reversal with piezoelectric wafer active sensors for structural health monitoring. *Journal of Nondestructive Evaluation*. 2007;**26**:123-134. DOI: 10.1007/s10921-007-0027-8
- [34] Clarke T, Simonetti F, Rohklin S, Cawley P. Development of a low-frequency high purity  $a(0)$  mode transducer for SHM application. *IEEE Transactions on Ultrasonics, Ferroelectrics, and Frequency Control*. 2009;**56**:68-1457. DOI: 10.1109/TUFFC.2009.1201
- [35] Liu ZH, Yu HT, He CF, Wu B. Delamination detection in composite beams using pure Lamb mode generated by air-coupled ultrasonic transducer. *Journal of Intelligent Material Systems and Structures*. 2014;**25**:541-550. DOI: 10.1177/1045389X13493339
- [36] Jayaraman C, Anto I, Balasubramaniam K, Venkataraman KS. Higher order modes cluster (HOMC) guided waves for online defect detection in annular plate region of above-ground storage tanks. *Insight - Non-destructive Testing and Condition Monitoring*. 2009;**51**:606-611. DOI: 10.1784/insi.2009.51.11.606
- [37] Khalili P, Cawley P. Excitation of single-mode Lamb waves at high-frequency-thickness products. *IEEE Transactions on Ultrasonics, Ferroelectrics, and Frequency Control*. 2016; **63**:12-303. DOI: 10.1109/TUFFC.2015.2507443
- [38] Guo ZQ, Achenbach JD, Krishnaswamy S. EMAT generation and laser detection of single Lamb wave modes. *Ultrasonics*. 1997;**35**:423-429. DOI: 10.1016/S0041-624X(97)00024-3
- [39] Lee JK, Kim YY. Tuned double-coil EMATs for omnidirectional symmetric mode reference Lamb wave generation. *NDT&E International*. 2016;**83**:38-47. DOI: 10.1016/j.ndteint.2016.06.001
- [40] Liu ZH, Hu YN, Xie MW, Wu B, He CF. Development of omnidirectional  $A_0$  mode EMAT employing a concentric permanent magnet pairs with opposite polarity for plate inspection. *NDT&E International*. 2018;**94**:13-21. DOI: 10.1016/j.ndteint.2017.11.001
- [41] Yoo B, Na SM, Flatau AB, Prines DJ. Directional magnetostrictive patch transducer based on Galfenol's anisotropic magnetostriction feature. *Smart Materials and Structures*. 2014; **23**:95035. DOI: 10.1088/0964-1726/23/9/095035
- [42] Khalili P, Cawley P. Relative ability of wedge coupled piezoelectric and meander coil EMAT probes to generate single mode Lamb waves. *IEEE Transactions on Ultrasonics, Ferroelectrics, and Frequency Control*. DOI: 10.1109/TUFFC.2018.2800296
- [43] Tomohiro Y, Uno Y. High-order Lamb waves for flaw detection in steel plates by electromagnetic acoustic transducers. *Journal of Solid Mechanics and Materials Engineering*. 2007;**1**:355-363. DOI: 10.1299/jmmp.1.355

- [44] Ostachowicz W, Radziński M, Kudela P. Comparison studies of full wavefield signal processing for crack detection. *Strain*. 2014;**50**:275-291. DOI: 10.1111/str.12098
- [45] Costley RD, Berthelot YH, Jacobs LJ. Fresnel arrays for the study of Lamb waves in laser ultrasonics. *Journal of Nondestructive Evaluation*. 1994;**13**:33-42. DOI: 10.1007/BF00723945
- [46] Song MK, Jhang KY. Crack detection in single-crystalline silicon wafer using laser generated Lamb waves. *Advances in Materials Science and Engineering*. 2013;**2013**:1-6. DOI: 10.1155/2013/950791
- [47] Huke P, Schröder M, Hellmers S, Kalms M, Bergmann RB. Efficient laser generation of Lamb waves. *Optics Letters*. 2014;**39**:5795-5797. DOI: 10.1364/OL.39.005795
- [48] Addison RC, Mckie ADW. Laser-based ultrasound arrays for generation and detection of narrowband single mode Lamb waves. In: *Proceedings of the 1994 IEEE Ultrasonics Symposium*; 01–04 November 1994; Cannes. New York: IEEE; 1994. pp. 1201-1404
- [49] Nakano H, Nagai S. Laser generation of antisymmetric Lamb waves in thin plates. *Ultrasonics*. 1991;**29**(3):230-234. DOI: 10.1016/0041-624X(91)90061-C
- [50] Todd MD, Johnson GA, Vohra ST. Deployment of a fiber Bragg grating-based measurement system in a structural health monitoring application. *Smart Materials and Structures*. 2001;**10**:534-539. DOI: 10.1088/0964-1726/10/3/316
- [51] Sicard R, Goyette J, Zellouf D. A numerical dispersion compensation technique for time recompression of Lamb wave signals. *Ultrasonics*. 2002;**40**:727-732. DOI: 10.1016/S0041-624X(02)00201-9
- [52] Wilcox PD. A rapid signal processing technique to remove the effect of dispersion from guided wave signals. *IEEE Transactions on Ultrasonics, Ferroelectrics, and Frequency Control*. 2003;**50**:419-427. DOI: 10.1109/TUFFC.2003.1197965
- [53] De Marchi L, Marzani A, Speciale N, Viola E. A passive monitoring technique based on dispersion compensation to locate impacts in plate-like structures. *Smart Materials and Structures*. 2011;**20**:35021. DOI: 10.1088/0964-1726/20/3/035021
- [54] De Marchi L, Marzani A, Miniaci M. A dispersion compensation procedure to extend pulse-echo defects location to irregular waveguides. *NDT and E International*. 2013;**54**: 115-122. DOI: 10.1016/j.ndteint.2012.12.009
- [55] Fu SC, Shi LH, Zhou YH, Cai J. Dispersion compensation in Lamb wave defect detection with step-pulse excitation and warped frequency transform. *IEEE Transactions on Ultrasonics, Ferroelectrics, and Frequency Control*. 2014;**61**:2075-2088. DOI: 10.1109/TUFFC.2014.006606
- [56] Xu KL, Ta DA, Hu B, Laugier P, Wang WQ. Wideband dispersion reversal of Lamb waves. *IEEE Transactions on Ultrasonics, Ferroelectrics, and Frequency Control*. 2014;**61**:997-1005. DOI: 10.1109/TUFFC.2014.2995
- [57] Xu BL, Yu LY, Giurgiutiu V. Lamb wave dispersion compensation in piezoelectric wafer active sensor phased-array applications. In: *Proceedings of the Conference on Health Monitoring of Structural and Biological Systems*, 8–12 March 2009, San Diego. California: SPIE Press; 2009. p. 7295: p. 729516. DOI: 10.1117/12.816085



- [58] Liu L, Yuan FG. A linear mapping technique for dispersion removal of Lamb waves. *Structural Health Monitoring*. 2010;**9**:75-86. DOI: 10.1177/1475921709341012
- [59] Cai J, Yuan SF, Wang TG. Signal construction-based dispersion compensation of Lamb waves considering signal waveform and amplitude spectrum preservation. *Materials*. 2016;**10**:4. DOI: 10.3390/ma10010004
- [60] Xu CB, Yang ZB, Chen XF, Tian SH, Xie Y. A guided wave dispersion compensation method based on compressed sensing. *Mechanical Systems and Signal Processing*. 2018;**103**:89-104. DOI: 10.1016/j.ymssp.2017.09.043
- [61] Alleyne DN, Pialucha TP, Cawley P. A signal regeneration technique for long range propagation of dispersive Lamb waves. *Ultrasonics*. 1993;**31**:201-204. DOI: 10.1016/0041-624X(93)90007-M
- [62] Zeng L, Lin J. Chirp-based dispersion pre-compensation for high resolution Lamb wave inspection. *NDT and E International*. 2014;**61**:35-44. DOI: 10.1016/j.ndteint.2013.09.008
- [63] Lin J, Hua JD, Zeng L, Luo Z. Excitation waveform design for lamb wave pulse compression. *IEEE Transactions on Ultrasonics, Ferroelectrics, and Frequency Control*. 2016;**63**:165-177. DOI: 10.1109/TUFFC.2015.2496292
- [64] Malo S, Fateri S, Livadas M, Mare C, Gan TH. Wave mode discrimination of coded ultrasonic guided waves using two-dimensional compressed pulse analysis. *IEEE Transactions on Ultrasonics, Ferroelectrics, and Frequency Control*. 2017;**64**:1092-1101. DOI: 10.1109/TUFFC.2017.2693319
- [65] Yücel MK, Fateri S, Legg M, Wikinson A, Kappatos V, Selcuk C, Gan TH. Coded waveform excitation for high resolution ultrasonic guided wave response. *IEEE Transactions on Industrial Informatics*. 2016;**12**:257-266. DOI: 10.1109/TII.2015.2501762
- [66] De Marchi L, Marzani A, Moll J, Kudela P, Radzienski M, Ostachowicz W. A pulse coding and decoding strategy to perform Lamb wave inspections using simultaneously multiple actuators. *Mechanical Systems and Signal Processing*. 2017;**91**:111-121. DOI: 10.1016/j.ymssp.2016.12.014
- [67] Hua JD, Lin J, Zeng L, Gao F. Pulse energy evolution for high-resolution Lamb wave inspection. *Smart Materials and Structures*. 2015;**24**:65016. DOI: 10.1088/0964-1726/24/6/065016
- [68] Xu KL, Ta D, Moilanen P, Wang WQ. Mode separation of Lamb waves based on dispersion compensation method. *The Journal of the Acoustical Society of America*. 2012;**131**:2714-2722. DOI: 10.1121/1.3685482
- [69] Agrahari JK, Kapuria S. Active detection of block mass and notch-type damages in metallic plates using a refined time-reversed Lamb wave technique. *Structural Control and Health Monitoring*. 2018;**25**:1-18. DOI: 10.1002/stc.2064
- [70] Zeng L, Lin J, Huang LP. A modified Lamb wave time-reversal method for health monitoring of composite structures. *Sensors*. 2017;**17**:955. DOI: 10.3390/s17050955

- [71] Huang LP, Zeng L, Lin J, Luo Z. An improved time reversal method for diagnostics of composite plates using Lamb waves. *Composite Structures*. 2018;**190**:10-19. DOI: 10.1016/j.compstruct.2018.01.096
- [72] Hong JC, Sun KH, Kim YY. The matching pursuit approach based on the modulated Gaussian pulse for efficient guided-wave damage inspection. *Smart Materials and Structures*. 2005;**41**:548-560. DOI: 10.1088/0964-1726/14/4/013
- [73] Le Touze G, Nicolas B, Mars JL, Lacoume JL. Matched representations and filters for guided waves. *IEEE Transactions on Signal Processing*. 2009;**57**:1783-1795. DOI: 10.1109/TSP.2009.2013907
- [74] Demirli R, Saniie J. Asymmetric Gaussian chirplet model and parameter estimation for generalized echo representation. *Journal of the Franklin Institute*. 2014;**351**:907-921. DOI: 10.1016/j.jfranklin.2013.09.028
- [75] Demirli R, Saniie J. Asymmetric Gaussian Chirplet model for ultrasonic echo analysis. In: *Proceedings of the 2010 IEEE International Ultrasonics Symposium Proceedings*; 11–14 October; California. New York: IEEE; 2010. pp. 124-128
- [76] Prosser WH, Seale MD, Smith BT. Time-frequency analysis of the dispersion of lamb modes. *The Journal of the Acoustical Society of America*. 1999;**105**:76-2669. DOI: 10.1121/1.426883
- [77] Kwok HK, Jones DL. Improved instantaneous frequency estimation using an adaptive short-time Fourier transform. *IEEE Transactions on Signal Processing*. 2000;**48**:2964-2972. DOI: 10.1109/78.869059
- [78] Pei SC, Huang SG. STFT with adaptive window width based on the chirp rate. *IEEE Transactions on Signal Processing*. 2012;**60**:4065-4080. DOI: 10.1109/TSP.2012.2197204
- [79] Chen B, Zhao SL, Li PY. Application of Hilbert-Huang transform in structural health monitoring: A state-of-the-art review. *Mathematical Problems in Engineering*. 2014. DOI: 10.1155/2014/317954
- [80] Guo W, Huang LJ, Chen C, Zuo HW, Liu ZW. Elimination of end effects in local mean decomposition using spectral coherence and applications for rotating machinery. *Digital Signal Processing*. 2016;**55**:52-63. DOI: 10.1016/j.dsp.2016.04.007
- [81] Xu BL, Giurgiutiu V, Yu LY. Lamb waves decomposition and mode identification using matching pursuit method. In: *Proceedings of SPIE, Sensors and Smart Structures Technologies for Civil, Mechanical, and Aerospace Systems 2009*; 27–30 March 2009; San Diego. Bellingham: SPIE Press; 2009. pp. 1-12
- [82] Demirli R, Saniie J. Asymmetric Gaussian chirplet model and parameter estimation for generalized echo representation. *Journal of the Franklin Institute-engineering and Applied Mathematics*. 2014;**351**:907-921. DOI: 10.1016/j.jfranklin.2013.09.028
- [83] Kim CY, Park KJ. Mode separation and characterization of torsional guided wave signals reflected from defects using chirplet transform. *NDT and E International*. 2015;**74**:15-23. DOI: 10.1016/j.ndteint.2015.04.006

- [84] Li FC, Su ZQ, Ye L, Meng G. A correlation filtering-based matching pursuit (CF-MP) for damage identification using Lamb waves. *Smart Materials and Structures*. 2006;**15**:1585-1594. DOI: 10.1088/0964-1726/15/6/010
- [85] Rostami J, Tse PWT, Fang Z. Sparse and dispersion-based matching pursuit for minimizing the dispersion effect occurring when using guided wave for pipe inspection. *Materials*. 2017;**10**:622. DOI: 10.3390/ma10060622
- [86] Mallat SG, Zhang ZF. Matching pursuits with time-frequency dictionaries. *IEEE Transactions on Signal Processing*. 1993;**41**:3397-3415. DOI: 10.1109/78.258082
- [87] Agarwal S, Mira M. Lamb wave based automatic damage detection using matching pursuit and machine learning. *Smart Materials and Structures*. 2014;**23**:85012. DOI: 10.1088/0964-1726/23/8/085012
- [88] Lu YF, Demirli R, Cardoso G, Saniie J. A successive parameter estimation algorithm for Chirplet signal decomposition. *IEEE Transactions on Ultrasonics, Ferroelectrics, and Frequency Control*. 2006;**53**:2121-2131. DOI: 10.1109/TUFFC.2006.152
- [89] Zeng L, Zhao M, Lin J, Wu WT. Waveform separation and image fusion for Lamb waves inspection resolution improvement. *NDT and E International*. 2016;**79**:17-29. DOI: 10.1016/j.ndteint.2015.11.006
- [90] Croxford AJ, Moll J, Wilcox PD, Michaels JE. Efficient temperature compensation strategies for guided wave structural health monitoring. *Ultrasonics*. 2010;**50**:28-517. DOI: 10.1016/j.ultras.2009.11.002
- [91] Clarke T, Simonetti F, Cawley P. Guided wave health monitoring of complex structures by sparse array systems influence of temperature changes on performance. *Journal of Sound and Vibration*. 2010;**329**:2306-2322. DOI: 10.1016/j.jsv.2009.01.052
- [92] Lu YH, Michaels JE. A methodology for structural health monitoring with diffuse ultrasonic waves in the presence of temperature variations. *Ultrasonics*. 2005;**43**:717-731. DOI: 10.1016/j.ultras.2005.05.001
- [93] Konstantinidis G, Wilcox PD, Drinkwater BW. An investigation into the temperature stability of a guided wave structural health monitoring system using permanently attached sensors. *IEEE Sensors Journal*. 2007;**7**:905-912. DOI: 10.1109/JSEN.2007.894908
- [94] Wang YS, Gao LM, Yuan SF, Qiu L, Qing XL. An adaptive filter-based temperature compensation technique for structural health monitoring. *Journal of Intelligent Material Systems and Structures*. 2014;**25**:2187-2198. DOI: 10.1177/1045389X13519001
- [95] Moll J, Fritzen CP. Guided waves for autonomous online identification of structural defects under ambient temperature variations. *Journal of Sound and Vibration*. 2012;**331**:4587-4597. DOI: 10.1016/j.jsv.2012.04.033
- [96] Clarke T, Simonetti F, Cawley P. Guided wave health monitoring of complex structures by sparse array systems influence of temperature changes on performance. *Journal of Sound and Vibration*. 2010;**329**:2306-2322. DOI: 10.1016/j.jsv.2009.01.052

- [97] Roy S, Lonkar K, Janapati V, Chang FK. A novel physics-based temperature compensation model for structural health monitoring using ultrasonic guided waves. *Structural Health Monitoring*. 2014;**13**:321-342. DOI: 10.1177/1475921714522846
- [98] Fendzi C, Rebillat M, Mechbal N, Guskov M, Coffignal G. A data driven temperature compensation approach for structural health monitoring using Lamb waves. *Structural Health Monitoring*. 2016;**15**:525-540. DOI: 10.1177/1475921716650997
- [99] Liu GQ, Xiao YC, Zhang H, Ren GX. Baseline signal reconstruction for temperature compensation in Lamb wave-based damage detection. *Sensors*. 2016;**16**:1273. DOI: 10.3390/s16081273
- [100] Dao PB, Staszewski WJ. Lamb wave based structural damage detection using cointegration and fractal signal processing. *Mechanical Systems and Signal Processing*. 2014;**49**:285-301. DOI: 10.1016/j.ymssp.2014.04.011